



Original article

Evaluation of peak-fitting software for magnesium quantification through k_0 -instrumental neutron activation analysis

Kishore B. Dasari^a, Hana Cho^b, Radojko Jaćimović^c, Byung-Gun Park^a,
Gwang-Min Sun^{a,*}

^a HANARO Utilization Division, Korea Atomic Energy Research Institute, Daejeon, 34057, Republic of Korea

^b Division of Chemical and Biological Metrology, Korea Research Institute of Standards and Science, Daejeon, 34113, Republic of Korea

^c Department of Environmental Sciences, Jožef Stefan Institute, 1000, Ljubljana, Slovenia



ARTICLE INFO

Article history:

Received 10 March 2021

Received in revised form

30 June 2021

Accepted 13 July 2021

Available online 14 July 2021

Keywords:

HyperLab

HyperGam

KayWin®

Magnesium

Peak deconvolution

Peak-fitting programs

ABSTRACT

The selection and effective utilization of peak-fitting software for conventional gamma-ray spectrum analysis is significant for accurate determination of the mass fraction of elements, particularly in complex peak regions. Majority of the peak-fitting programs can derive similar peak characteristics for singlet peaks, but very few programs can deconvolute multi-peaks in a complex region. The deconvolution of multi-peaks requires special peak-fitting functions, such as left and right-skew distributions. In the this study, 843.76 keV (^{27}Mg) peak area from the complex region (840 keV–850 keV) determined and compared using four different peak-fitting programs, namely, GammaVision, Genie2000, HyperLab, and HyperGam. The 843.76 keV peak interfered with 841.63 keV ($^{152\text{m}}\text{Eu}$) and 846.81 keV (^{56}Mn). The total Mg concentration was determined through k_0 -instrumental neutron activation analysis by applying the isotopic interference correction factor $^{27}\text{Al}(n,p)^{27}\text{Mg}$ through the simultaneous determination of Al concentration. HyperLab and HyperGam peak-fitting programs reported consistent peak areas, and resultant concentrations agreed with the certified values of matrix-certified reference materials.

© 2021 Korean Nuclear Society, Published by Elsevier Korea LLC. This is an open access article under the CC BY-NC-ND license (<http://creativecommons.org/licenses/by-nc-nd/4.0/>).

1. Introduction

Magnesium (Mg) is an essential nutrient element in human and plant biological systems. It helps in maintaining normal human body functions, such as the muscular, nervous, and immune systems, along with healthy plant growth [1]. Mg deficiency is linked to numerous diseases in the human body, such as hypertension [2]. Thus, the characterization of Mg-rich diets and the total mass fraction of Mg in various biological and environmental samples is important. Among the dry and wet chemistry analytical techniques, non-destructive methods are preferred in the analysis of aerosol particles and biological samples to avoid chemical contamination during the rigorous process of sample preparation.

Neutron activation analysis (NAA) is an outstanding technique that is non-destructive, highly sensitivity, and has a lower detection limit. The comparator INAA method is a unique primary calibration method with dry chemical analysis [3]. Apart from the comparator

INAA method, the k_0 -based single comparator INAA (k_0 -INAA) method has considerable characteristics for the determination of mass fraction of elements in various matrix samples and reference material development [4–6]. The k_0 -INAA method also competes with other primary ratio methods for inorganic trace element quantification [4]. However, some elements (Mg, Sm, and Sr) cannot be determined accurate mass fraction because of issues such as short half-life of activation products, gamma-ray, and isotopic interferences [7]. In INAA, total Mg content is determined using $^{26}\text{Mg}(n,\gamma)^{27}\text{Mg}$ (843.76 keV and 1014.44 keV) reaction that is interfered with by gamma-rays of 841.63 keV ($^{152\text{m}}\text{Eu}$) and 846.81 keV (^{56}Mn) to 843.76 keV gamma-line, and nuclear reaction interference from $^{27}\text{Al}(n,p)^{27}\text{Mg}$. Most of the environmental and biological samples contain Mg and interference elements such as Mn, Eu, and Al with high concentration. The complete avoidance of possible spectral and isotopic interference in the INAA method is impossible. The k_0 -INAA method is preferred over the comparator

* Corresponding author.

E-mail address: gmsun@kaeri.re.kr (G.-M. Sun).

INAA method for Mg quantification because the isotopic corrections can be calculated easily when both the analyte and interference elements are determined simultaneously [6].

Mg has three stable isotopes: Mg-24 (79%), Mg-25 (10%), and Mg-26 (11%). ^{26}Mg has a (n,γ) cross-section (σ_0) of 0.0364 b, and neutron-induced ^{27}Mg has a short half-life of 9.46 m and emits three gamma-rays, 170.69 keV (γ_a : 0.8%), 843.76 keV (γ_a : 71.8%), and 1014.44 keV (γ_a : 28.0%) that, which are suitable for the calculation of the total Mg content through INAA. However, Mg quantification using 843.76 keV peak has two primary issues: gamma-ray interferences and isotopic interference. The Mg mass fraction is more than 10 times the interference elements (Eu and Mn) in most of the samples, although significant gamma-ray interference was caused by the relatively high thermal neutron cross section and abundance of gamma-rays of interference elements. Nuclear data was obtained from the radionuclide decay database online library for gamma and alpha emissions (<http://www.nucleide.org/Laraweb/index.php>) and k_0 -database [8]. ^{27}Mg emits another interference free gamma-ray at 1014.44 keV with only 30% of the 843.76 keV peak intensity and is subject to large uncertainty because of poor counting statistics. Thus, identifying suitable peak-fitting software for two or more gamma-ray interference regions is necessary to obtain more reliable peak areas with corresponding uncertainties. In this study, both the peak areas of ^{27}Mg (843.76 keV and 1014.44 keV) were used to determine the total Mg mass fraction. In addition to gamma-ray interference, isotopic interference from the (n,p) threshold reaction in aluminum (Al) caused by the fast neutrons was also considered. If the sample contains high amounts of Al, Mg mass fraction likely bias because of isotopic interference from the $^{27}\text{Al}(n,p)^{27}\text{Mg}$ reaction [5,7]. Another isotopic threshold interference from $^{30}\text{Si}(n,\alpha)^{27}\text{Mg}$ did not significant contribute to the total Mg content because of the low abundance of silicon isotope (3.1%) and low (n,α) cross-section (0.155 mb). These isotopic issues can be solved by introducing an isotopic correction factor such as the auto-correction option implemented in the revised version of the KayWin® software [6,9,10].

In 1995, the International Atomic Energy Agency (IAEA) conducted an inter-comparison study using synthetic gamma-ray spectra to identify a suitable peak-fitting program for gamma-ray spectrum analysis in terms of the number of peaks, peak position, peak position error, full width at half maximum (FWHM), peak area, peak-fitting error, and Chi-square [11]. Based on the findings, most of the programs were suitable for single-peak characterization and not recommended for complex peak region analysis, where there were two or more gamma-ray interferences [11]. Some programs such as Ganaas, Hypermet PC, GammaVision, Genie PC, and Span have shown consistent peak characterization in the complex region [11]. However, most of the peak-fitting programs are not compatible with personal computer (PC) versions, such as Windows 7 (issued in 2009) operating systems (OS) except

GammaVision and Genie PC (updated as Genie2000), because they were not upgraded in a timely manner. Meanwhile, several programs have been developed, including HyperLab, HyperGam, and Gammalab that compatible with the present Windows OS. Some of these programs, such as HyperLab and HyperGam, were developed based on the Hypermet code [12,13]. In most software, FWHM calibration is used for deconvolution of the merged peaks. However, one peak may have high peak intensity while another closer peak on the left or right-side has a low peak intensity that will be considered as tails. To resolve this issue and identify the low peak intensity gamma-ray on the left or right-side of the high-intensity peak requires special peak-fitting functions such as left or right-skew functions. In recently developed programs also did not find satisfactory discussions on complex peak region analysis using IAEA synthetic or experimental gamma-ray spectra [12,14,15].

The aim of the present study is to identify suitable deconvolution capability of peak fitting program for the complex region using four software programs GammaVision, Genie2000, HyperLab, and HyperGam. Subsequently, the peak area was used for mass fraction determination in various matrix certified reference materials. Isotopic interference correction factor also calculated for the determination of Mg mass fraction accurately using k_0 -INAA method. In the present study, four different matrix certified reference material (CRM) samples, urban particulate matter (NIST SRM 1648a), infant formula (KRIS CRM 108-02-004), peach leaves (NIST SRM 1547), and channel sediment (BCR-320R), were analyzed for the determination of total Mg and Al mass fractions simultaneously.

2. Theory

The software identifies the peaks on the basis of various functions such as peak type (Gaussian, FWHM, left-skew, and right-skew) and background type (polynomial, step, and tail) functions [16,17]. In this study, the peak type model functions required for the deconvolution of complex region gamma-rays are briefly discussed. The following peak functions are important for the analysis of complex region gamma-rays.

Gaussian peak function: The peak area of the Gaussian peak is calculated using Equation (1), which is a symmetry function (Fig. 1(a)). All peak-fitting programs consider this function to be important for singlet peak area calculations.

$$\text{Gaussian peak function} = \psi \cdot e^{-\left(\frac{x-x_0}{\delta}\right)^2}, \quad (1)$$

where x and x_0 represent the channel number and centroid of the peak position, respectively, ψ represents the amplitude of the peak, and δ represents the peak width parameter (FWHM/1.66).

Left-skew function: Some peaks appear as asymmetric shapes with an exponential decrease in the low-energy side from the

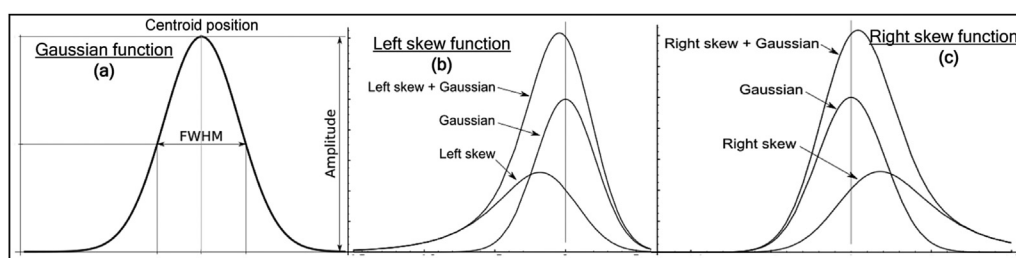


Fig. 1. Semi-empirical model functions of (a) Gaussian distribution, (b) Gaussian + left-skew, and (c) Gaussian + right-skew [17].

centroid of the Gaussian peak. This slope may be due to weak gamma peak energy (in terms of intensity) on the low-energy side (left-skew + Gaussian peak), as shown in Fig. 1(b). This low-energy peak can be easily resolved using the left-skew function (Equation (2)). In some cases, the asymmetric shape of the Gaussian peak may also be due to incomplete charge collection (tail background) in the detector. These two functions can be separated by a slope term. The tail background slope is 2.5–50, whereas the left-skew function slope ranges 0.3–2. Few software programs (e.g., HyperLab and Hypermet PC) consider this function for better deconvolution of merged peaks [16,17].

$$\text{Left skew function} = \psi \cdot \frac{\sqrt{\pi}}{2} \cdot \delta \cdot \alpha \cdot e^{\left(\left[\frac{\delta}{2\alpha_1} \right]^2 + \frac{x-x_0}{\alpha_1} \right) \cdot \text{erfc} \left(\frac{\delta}{2\alpha_1} + \frac{x-x_0}{\delta} \right)}, \tag{2}$$

where α denotes the left-skew amplitude relative to Gaussian, α_1 denotes the left-skew slope (0.3–0.2), and erfc denotes the standard complementary error function ($\text{erfc}(x) = 1 - \frac{2}{\sqrt{\pi}} \int_0^x e^{-t^2} dt$).

Right-skew function: The right-skew function is similar to the left-skew function form at the right side of the Gaussian peak, where they mirror each other. Fig. 1(c) shows a right-skewed function with at Gaussian peak. This high-energy peak with a low peak area can be resolved using the right-skewed function (Equation (3)). The Gaussian peak appears as an asymmetric shape with an exponential decrease in the right high-energy side from the centroid of the Gaussian peak. Similar to the left-skew function, this skewness function is also important for the deconvolution of complex regions. In some cases, right-skewness feature appears because of pile-up effect, particularly it is appearing in short-lived

radionuclide and high dead-time counting measurement. These two functions can be separated using a slope term as mentioned in the left-skew function. Based on the information given in the peak-fitting software manuals, this function was included in the recently developed peak-fitting programs such as HyperLab [17]. However, it was not considered in the original Hypermet PC code [16]. These three functions play an important role in the deconvolution of merged peaks along with the background functions [17]. Another suitable application of the right-skew function are ^{85}Sr (514.0 keV), it is right side of the annihilation peak (511.0 keV), and ^{65}Zn (1115.54 keV).

$$\text{Right skew function} = \psi \cdot \frac{\sqrt{\pi}}{2} \cdot \delta \cdot \beta \cdot e^{\left(\left[\frac{\delta}{2\beta_1} \right]^2 - \frac{x-x_0}{\beta_1} \right) \cdot \text{erfc} \left(\frac{\delta}{2\beta_1} - \frac{x-x_0}{\delta} \right)}, \tag{3}$$

where β denotes the right-skewed amplitude relative to Gaussian, β_1 represents the right-skewed slope (0.3–0.2), and erfc denotes the standard complementary error function.

3. Experimental details

The samples were pressed into standard geometry pellets (\varnothing 13 and 1 mm thicknesses) using a Whatman® cellulose filter paper to minimize the correction factors of neutron absorption, scattering, and gamma-ray attenuation. IRMM-530R Al-0.1%Au alloy foil (thickness: 0.1 mm) was used as the flux monitor and comparator. The samples and flux monitors were heat-sealed with polyethylene. Samples were irradiated with approximate thermal and epithermal neutron flux of $1.1 \times 10^{12} \text{ cm}^{-2} \text{ s}^{-1}$ and $3.6 \times 10^{10} \text{ cm}^{-2} \text{ s}^{-1}$, respectively, at the TRIGA Mark II nuclear

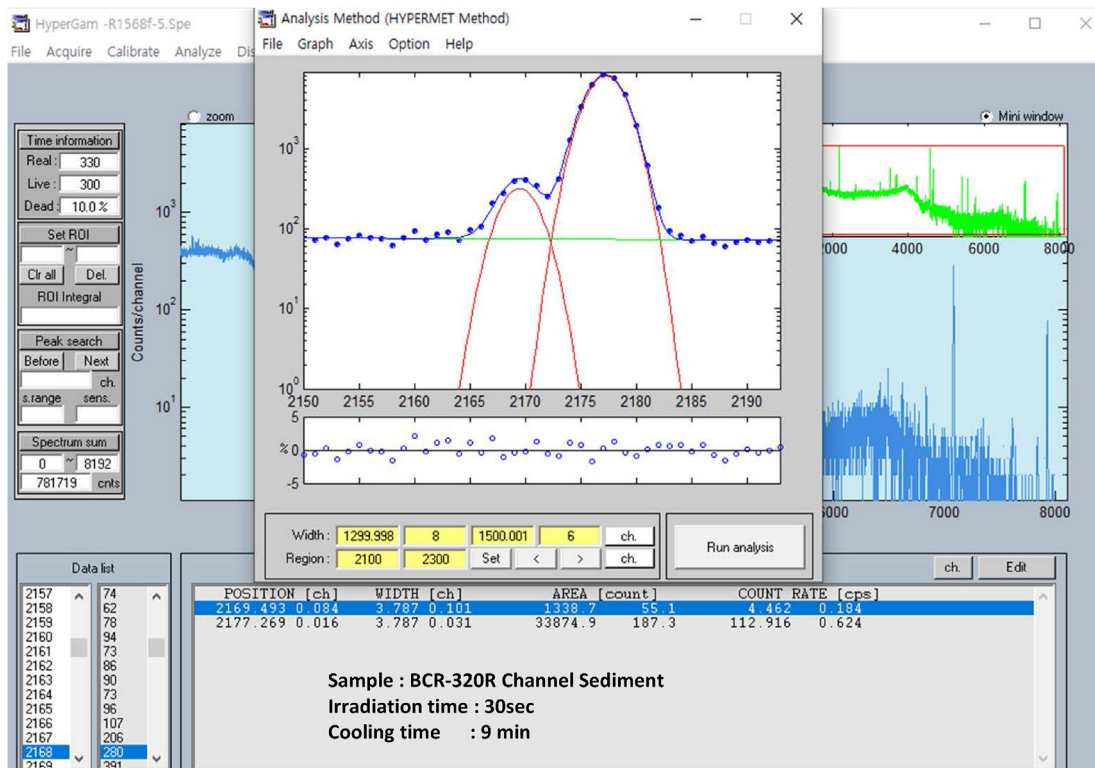


Fig. 2. Deconvolution of the complex region containing 843.76 keV (^{27}Mg) and 846.81 keV (^{56}Mn) with HyperGam program (BCR-320R channel sediment).

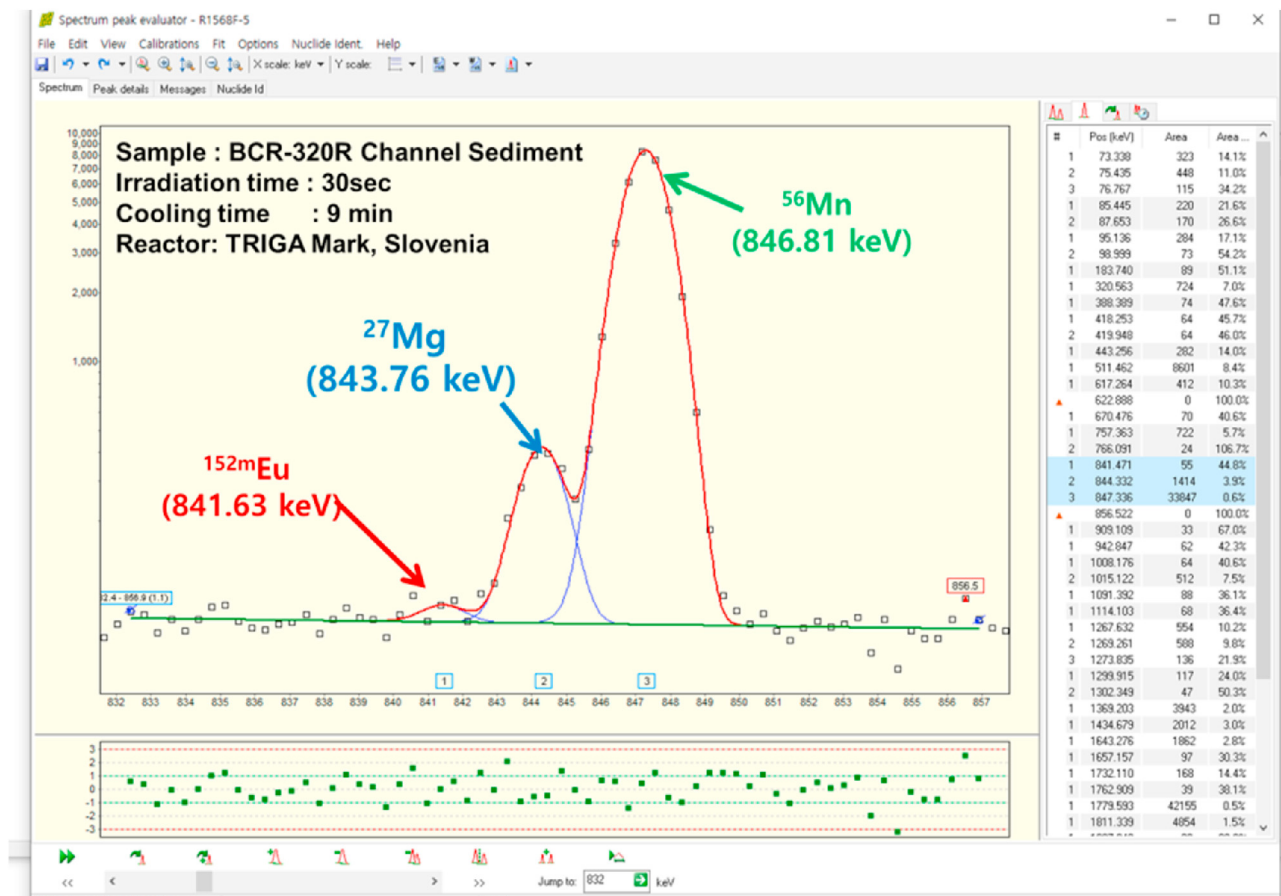


Fig. 3. Deconvolution of the complex region containing 841.63 keV (^{152m}Eu), 843.76 keV (²⁷Mg), and 846.81 keV (⁵⁶Mn) with HyperLab program (BCR-320R channel sediment).

reactor, Jožef Stefan Institute, Ljubljana, Slovenia, for 30 s for determination of short-lived radionuclides. After an appropriate cooling time (<10 min), the samples were transferred to a radioactive laboratory for offline gamma-ray measurement using a high-resolution HPGe detector (45% relative efficiency and 1.8 keV FWHM at 1332 keV) with <10% dead time. The short-lived radionuclide gamma-ray spectra were obtained at a distance of 20 cm from the detector and a 300 s time measurement using Maestro software with the zero dead time (ZDT) counting mode. The ZDT achieved a good performance for real-time correction in the peak area up to 30% dead time, including variable dead time during the short-lived radionuclide measurement [18]. Four different automatic peak-fitting programs, namely, HyperLab ver2014.1 [17], HyperGam ver1.3 [12,19], GammaVision ver6.01 [20], and Genie2000 ver3.1 [21] were used to analyze and compare the peak area of short-lived radionuclides (Mg and Al). The HyperLab peak report was used for concentration determination using the *k*₀-INAA method with KayWin® software [10]. More details on the experimental conditions, procedure, and calculations are provided in previous articles [5,22,23].

4. Results and discussion

4.1. Determination of peak areas using different peak-fitting software

The deconvolution of the merged peaks in the conventional gamma-ray spectrum using commercially available software was performed. All four software programs resolved the merged peak

areas along with uncertainties of the 843.76 keV (²⁷Mg) and 846.81 keV (⁵⁶Mn) gamma-rays except for GammaVision. GammaVision could not identify the 843.76 keV peak and merged it the 846.81 keV peak. Although the 843.76 keV peak area was determined through collectively peak evaluation process using interactive in viewed area mode instead of peak fitting. Screen shots of the peak-fitting analysis of the HyperGam and HyperLab programs for the BCR-320R channel sediment are presented in Figs. 2 and 3, respectively. As shown in Fig. 2 and 843.76 keV fitted slightly off with HyperGam to the original fitting because it cannot identify low-energy peaks at 841.63 keV (^{152m}Eu). HyperLab can identify the third peak at 841.63 keV with a small peak area (Fig. 3) in the complex region, and this peak is not available in the HyperGam and Genie2000 programs. Along with complex region peak area analysis, singlet peak areas at 1014.44 keV (²⁷Mg) and 1778.97 keV (²⁸Al, half-life 2.24 m) were also determined for the quantification of Mg and Al. The capability of peak area determination was tested using statistical parameters, z-score, and percentage (%) deviation with respect to the reference peak report. In this study, the HyperLab peak report was considered as the reference spectra and peak areas that were used for total element concentration determination using *k*₀-INAA. The % deviation and z-score values were determined using Equations (4) and (5), respectively.

$$Dev. (\%) = \frac{x_i - x_j}{x_j} \cdot 100 \% \tag{4}$$

Table 1 Results of percentage (%) deviation and z-score for peak area with respect to the HyperLab peak areas of different peak-fitting programs for Mg and Al. HyperLab peak areas are reported along with fitting error percentage in parenthesis.

Sample	HyperLab			HyperGam			Genie2000			GammaVision											
	²⁷ Mg, E _γ (1) % dev. z	²⁷ Mg, E _γ (2) % dev. z	²⁸ Al, E _γ (1) % dev. z	²⁷ Mg, E _γ (1) % dev. z	²⁷ Mg, E _γ (2) % dev. z	²⁸ Al, E _γ (1) % dev. z	²⁷ Mg, E _γ (1) % dev. z	²⁷ Mg, E _γ (2) % dev. z	²⁸ Al, E _γ (1) % dev. z												
Urban PMs	2306(5.5%)	897(5.3%)	40,666(0.5%)	1.08	0.17	4.79	0.63	1.34	1.51	30.1	3.38	10.8	0.73	0.93	1.30	16.7	NC	5.94	0.41	0.68	0.94
Infant formula	1012(2.6%)	411(5.2%)	122(11.9%)	1.58	0.35	7.54	0.79	10.0	0.42	15.8	2.48	-6.08	-0.41	65.6	1.45	11.0	NC	-6.57	-0.61	-20.5	-0.46
Peach leaves	8383(0.9%)	2834(1.5%)	9766(0.8%)	-2.09	-1.21	-1.27	-0.34	0.97	0.68	0.17	0.09	-1.27	-0.42	0.59	0.44	4.47	NC	-1.06	-0.39	1.22	0.89
Channel Sediment	1258(5.5%)	520(7.2%)	42,182(0.5%)	7.23	1.02	3.85	0.34	-0.24	-0.31	36.0	4.17	0.38	0.04	0.18	0.21	4.61	NC	-3.65	-0.34	0.12	0.16

NC: not calculated because of GammaVision program not generated peak fitting error (manually fitted deconvolution peaks); ²⁷Mg, E_γ(1) = 843.76 keV, ²⁷Mg, E_γ(2) = 1014.44 keV, ²⁸Al, E_γ(1) = 1778.97 keV.

$$z = \frac{x_i - x_j}{\sqrt{\sigma_i^2 + \sigma_j^2}} \tag{5}$$

where x_i and x_j denote the peak areas reported by specific and reference software (HyperLab), and σ_i and σ_j represent peak-fitting errors reported by specific and reference software, respectively.

All selected programs yield the same fitting results of FWHM, peak position, and peak position uncertainty with $\pm 2\%$ deviation, except for peak areas. The peak areas reported by the HyperLab and HyperGam programs are close values than those reported by the Genie2000 and GammaVision programs. The 1778.97 keV peak fitting error for infant formula is high because of the low peak area or low concentration. The % deviation and z-score of the peak area fitting calculated in HyperGam, Genie2000, and GammaVision with regard to HyperLab are summarized in Table 1. The % deviation and z-score values of HyperGam are within $\pm 10\%$ and $\leq \pm 2$, respectively, which are close to the HyperLab values. The HyperGam and HyperLab programs were developed based on Hypermet-PC code. Thus, the peak search functions of these two programs were similar. Moreover, additional peak-fitting functions, such as the right-skew function, were included in HyperLab, which are not in the basic Hypermet-PC and HyperGam [16]. This right-skewed function is significant for the deconvolution of two or more peaks in the integrated region. The results from the other two programs, namely, Genie2000 and GammaVision, were inconsistent with HyperLab peak characteristics, and most of the peak area results had more than $\pm 10\%$ deviation and were out of the ± 2 z-score range. In GammaVision, the z-score was not calculated for the 843.76 keV peak because fitting errors were not reported. The four selected peak fitting programs were arranged according to their deconvolution capability under the present experimental and measurement conditions: HyperLab, HyperGam, Genie2000, and GammaVision.

4.2. Determination of magnesium concentration through k_0 -based INAA

The simultaneous determination of Mg using two major gamma-ray peak areas (843.76 keV and 1014.44 keV) and Al in different matrix CRM samples was performed through k_0 -INAA. In KayWin® software, the weighted mean mass fraction (ρ) of the analyte (a) along with the observed (obs) and expected (exp) uncertainty are calculated using Equations (6)–(8) that provide more reliable information about the quality of the results [6,10]. In this software, the counting statistics of peak-fitting were not considered because the counting statistics of all peak areas were not reliable in all cases. A typical analyte mass fraction determination, including the isotopic interference correction factor calculation using KayWin® software (k_0 -INAA), is shown in Fig. 4.

$$\rho_a = \frac{\sum_{i=1}^n \rho_i w_i}{\sum_{i=1}^n w_i} \tag{6}$$

$$\sigma_{i,obs} = \sqrt{\frac{\sum_{i=1}^n w_i (\rho - \rho_i)^2}{(n - 1) \sum_{i=1}^n w_i}} \tag{7}$$

$$\sigma_{i,exp} = \sqrt{\frac{\sum_{i=1}^n (w_i \sigma_i)^2}{(\sum_{i=1}^n w_i)^2}} \tag{8}$$

where $w_i = \frac{1}{\sigma_i^2}$ represents the weighting factor of a particular gamma-line (i), and ρ_i represents the weighted mean mass fraction

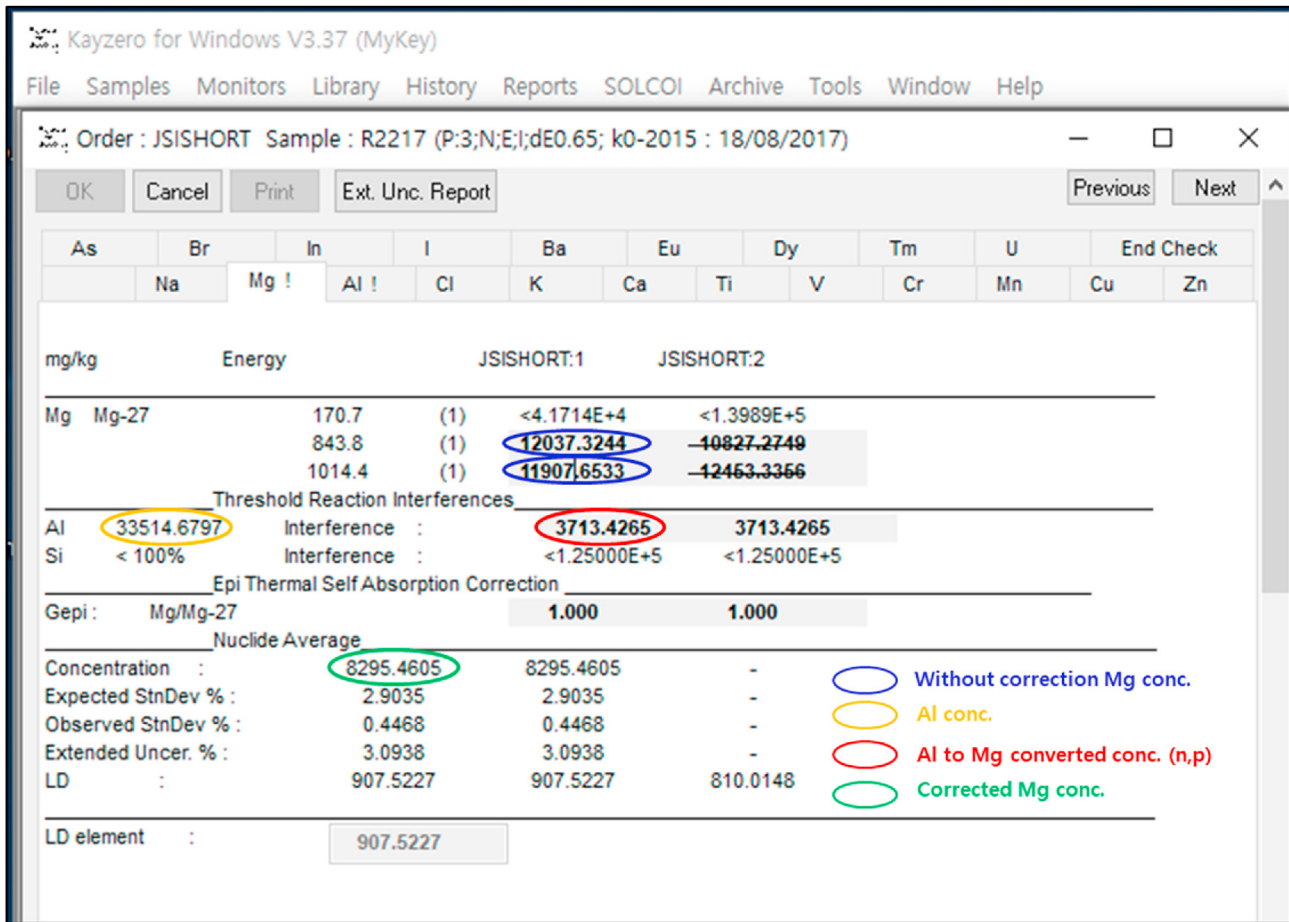


Fig. 4. Calculation of Mg concentration through auto correction of threshold reaction interferences using KayWin® software.

of a particular gamma-line.

The combined standard uncertainty with a coverage factor at $k = 1$ and expanded uncertainty (U) at $k = 2$ (95% confidence interval) of the final result was calculated using Equations (9) and (10).

$$u_{c,a} = \sqrt{u_{AREA,corr}^2 + u_{a,method}^2} \tag{9}$$

$$U_a = 2 \cdot u_{c,a} \tag{10}$$

where $u_{AREA, corr}$ denotes the uncertainty of the corrected net peak area, and u_{method} represents the overall standard uncertainty of the k_0 -INAA method (approximately 3.5%) that take into account the contribution from k_0 -factors, f , α , Q_0 , ϵ_p , and true coincidence effects [6,10].

The results, which show the expanded uncertainties with a coverage factor of $k = 2$, are summarized in Table 2. The expanded uncertainty using a gamma-ray energy of 843.76 keV is within $\pm 8\%$ that is lower than the expanded uncertainty using 1014.44 keV ($\pm 12\%$). The Mg concentration with 843.76 keV is a more reliable value with a lower uncertainty than with 1014.44 keV. However, part of the Mg concentration was contributed by Al because of the fast neutron nuclear reaction $^{27}\text{Al}(n,p)^{27}\text{Mg}$. Approximately 11% Al was converted into Mg during sample irradiation in the irradiation channel (IC-40) of the 250 kW TRIGA Mark II reactor, where all irradiations were performed. The conversion factor for isotope interference nuclides depends on the fast neutron flux in the

irradiation position and it determined experimentally [24] using an Al-0.1%Au alloy (IRMM-530R) with approximately 99.9% of Al. The variation of the neutron flux in the sample irradiation position was monitored using an Al-0.1%Au alloy and irradiated along with the sample. Consequently, the determination of the accurate concentration of isotopic interference of Mg through the standard comparator INAA becomes difficult. This issue can be solved easily by the k_0 -INAA method using KayWin® software that which includes an isotopic correction factor. However, it is possible only the analyte and interference elements analyzed simultaneously. The quality of laboratory values is compared with certified values through E_n -score that is calculated using Equation (11) [23].

$$E_n = \frac{X_{lab} - X_{ref}}{\sqrt{U_{lab}^2 + U_{ref}^2}} \tag{11}$$

where X_{lab} and X_{ref} denote the laboratory and reference values, and U_{lab} and U_{ref} represent the expanded uncertainties ($k = 2$) of the laboratory and reference values, respectively.

The experimental mass fraction values were consistent with the certified values, and the % deviations and E_n -scores were 6% and ≤ 1 with satisfactory results, respectively, except for Al in the infant formula sample. The concentration of Al in infant formula samples is low (< 1 mg/kg) and, may be easily in-homogenized owing to contamination from the sample wrapping materials. The Mg mass fraction value was determined by 843.76 keV gamma-rays that were more consistent with the certified values compared with

Table 2

Results for Mg and Al mass fraction obtained through k_0 -INAA in different CRMs. Results are given in mg/kg (dry mass basis) with associated expanded uncertainties ($k = 2$) along with % deviation and E_n -score.

Sample	Certified value (Mg)	Mg: ^{27}Mg , $E_\gamma(1)$			Mg: ^{27}Mg , $E_\gamma(2)$			Mg: ^{27}Mg , $E_\gamma(1)$ and $E_\gamma(2)$			Certified value	Al: ^{28}Al , $E_\gamma(1)$		
		This work	% dev.	E_n	(Al)	% dev.	E_n	This work	% dev.	E_n		This work	% dev.	E_n
Urban PMs	8130 ± 120	8436 ± 791	3.76	0.38	8314 ± 1217	2.26	0.15	8415 ± 750	3.51	0.38	34,300 ± 1300	33,966 ± 2433	−0.97	−0.12
Infant formula	582.7 ± 8.1	559 ± 49	−4.00	−0.47	676 ± 84	15.9	1.11	577 ± 92	−1.03	−0.07	0.79 ± 0.28	3.30 ± 0.82	318	2.91
Peach leaves	4320 ± 150	4546 ± 326	5.23	0.63	4579 ± 347	5.99	0.68	4557 ± 304	5.49	0.70	248.9 ± 6.5	265 ± 20	6.36	0.77
Channel Sediment	NA	6563 ± 862	NC	NC	8182 ± 1545	NC	NC	6869 ± 965	NC	NC	NA	32,110 ± 2259	NC	NC

NC: not calculated; NA: not available; ^{27}Mg , $E_\gamma(1) = 843.76$ keV, ^{27}Mg , $E_\gamma(2) = 1014.44$ keV, ^{28}Al , $E_\gamma(1) = 1778.97$ keV.

1044.44 keV gamma-rays owing to the high weighted mean uncertainty. If the Mg concentration is high (~1%), then we can use both the gamma-ray peak areas. In contrast, in the case of low Mg content, using the 843.76 keV gamma peak area determined by HyperLab or HyperGam was recommended instead of 1014.44 keV. However, these findings depend on the intensity of the 846.81 keV (^{56}Mn) peak next to it. Based on the present observation, the Mg peak area should be more than 5% with regard to the strongest peak at 846.81 keV.

5. Conclusions

In this study, the Mg mass fraction was determined accurately using 843.76 keV gamma-ray through k_0 -INAA in different matrix samples. In nonlinear peak fitting functions, the Gaussian peak, left-skew, and right-skew functions are important for the deconvolution of the merged peaks. The four peak-fitting programs, namely, HyperLab, HyperGam, Genie2000, and GammaVision were used for complex region analysis and compared. The best peak area fitting program in the selected programs according to this study is as follows: HyperLab, HyperGam, Genie2000, and GammaVision. Among the programs, HyperLab and HyperGam exhibited better fitting characteristics of closely integrated peaks with low residuals. Moreover, the right-skew function included HyperLab program can extend also in complex cases of ^{85}Sr (514.00 keV) and ^{65}Zn (1115.54 keV), where these gamma lines are affected by the annihilation gamma-ray (511.0 keV) and ^{152}Eu (1112.08 keV), ^{46}Sc (1120.54 keV), respectively. The nuclear interference factor caused by $^{27}\text{Al}(n,p)^{27}\text{Mg}$ was considered to affect the total Mg content. The combination of HyperLab and KayWin® programs for k_0 -INAA is recommended for the accurate quantification of elements with gamma-ray and isotopic interferences.

Declaration of competing interest

The authors declare that they have no known competing financial interests or personal relationships that could have appeared to influence the work reported in this paper.

Acknowledgement

The authors from KAERI & KRISS thank Prof. Milena Horvat, Head of the Department of Environmental Sciences at JSI, for her support of the experimental work at JSI funded by the Slovenian Research Agency (ARRS) programme P1-0143 and the Metrology Institute of the Republic of Slovenia (MIRS), Slovenia contract No. C3212-10-000071 (6401-5/2009/27). This work was supported by KAERI, South Korea through the Korea Government project No. MSIT/1711078081, 2021. This work was also supported by KRISS, South Korea under the project, "Establishment of Measurement Standards for Inorganic Analysis" Grant No. 21011058, 2021.

References

- [1] J.-D. Wilhelm, K. Markus, Magnesium basics, Clin. Kidney J. 5 (2012) i3–i14.
- [2] L.J. Dominguez, N. Veronese, M. Barbagallo, Magnesium and hypertension in old age, Nutrients 13 (2021) 139.
- [3] R.R. Greenberg, P. Bode, E.A. De Nadai Fernandes, Neutron activation analysis: a primary method of measurement, Spectrochim. Acta B 66 (3–4) (2011) 193–241.
- [4] R. Jaćimović, B. Smodiš, T. Bučar, P. Stegnar, k_0 -NAA quality assessment by analysis of different certified reference materials using the KAYZERO/SOLCOI software, J. Radioanal. Nucl. Chem. 257 (3) (2003) 659–663.
- [5] H. Cho, K.B. Dasari, R. Jaćimović, R. Zeisler, N.E. Sharp, S.-H. Kim, G.-M. Sun, Y.-H. Yim, Application of the INAA methods for KRISS infant formula CRM analysis: standardization of INAA at KRISS, J. Radioanal. Nucl. Chem. 322 (2019) 1537–1547.
- [6] F. De Corte, The K_0 -Standardization Method: a Move to the Optimization of Neutron Activation Analysis, Habilitation Thesis, University of Gent, Belgium, 1987.
- [7] G. Kennedy, J.-L. Galiniera, L. Zikovskiy, Measurement of some primary nuclear interferences in neutron activation analysis with a SLOWPOKE reactor, Can. J. Chem. 64 (1986) 790–792.
- [8] k_0 Database, 2020. http://www.kayzero.com/k0naa/k0naaorg/Nuclear_Data_SC/Entries/2020/8/24_Update_of_k0-database_I-128.html. Accessed 02 January 2021.
- [9] F. De Corte, A. Simonits, Vade Mecum for K_0 -Users, DSM Research, Geleen, 1994.
- [10] User's Manual for reactor neutron activation analysis (NAA) using the k_0 standardization method, in: Kayzero for Windows (KayWin®) Version 3.30, 2017.
- [11] M. Blaauw, V. Osorio Fernandez, P. van Espen, G. Bernasconi, R. Capote Noy, H. Manh Dung, N.I. Molla, The 1995 IAEA intercomparison of γ -ray spectrum analysis software, Nucl. Instrum. Methods A 387 (1997) 416–432.
- [12] B.-G. Park, H.D. Choi, C.S. Park, New development of hyperGam and its test of performance for γ -ray spectrum analysis, Nucl. Eng. Technol. 44 (2012) 781–790.
- [13] A. Simonits, J. Östör, S. Kálvin, B. Fazekas, HyperLab: a new concept in gamma-ray spectrum analysis, J. Radioanal. Nucl. Chem. 257 (2003) 589–595.
- [14] J.M. Los Arcos, M. Blaauw, S. Fazinic, V.P. Kolotov, The 2002 IAEA test spectra for low-level γ -ray spectrometry software, Nucl. Instrum. Methods A 536 (2005) 189–195.
- [15] C.A. Kalfas, M. Axiotis, C. Tsabaris, SPECTRW: a software package for nuclear and atomic spectroscopy, Nucl. Instrum. Methods A 830 (2016) 265–274.
- [16] L. Szentmiklosi, Fitting special peak shapes of prompt gamma spectra, J. Radioanal. Nucl. Chem. 315 (2018) 663–670.
- [17] HyperLab User's Manual for Gamma Spectroscopy Software, 2014. <http://www.hlabsoft.com/web/hl2014/online/docs.php>. accessed 15 February, 2021.
- [18] R. Acharya, K.B. Dasari, D. Chandra Shekhar, P.K. Pujari, Performance of digital gamma ray spectrometer for loss free counting and its application to NAA using short-lived radionuclides, J. Radioanal. Nucl. Chem. 302 (2014) 1333–1337.
- [19] C.S. Park, H.D. Choi, G.M. Sun, J.H. Whang, Status of developing HPGe γ -ray spectrum analysis code HYPERGAM, Prog. Nucl. Energy 50 (2008) 389–393.
- [20] GammaVision Gamma Spectroscopy Software User's Manual, 2016. <https://www.ortec-online.com/products/application-software/gammavision>.
- [21] Genie2000 Basic Spectroscopy Software User's Manual, 2006. <https://www3.nd.edu/~wzech/Genie%202000%20Operations%20Manual.pdf>.
- [22] H. Cho, K.B. Dasari, M.C. Lim, G.M. Sun, R. Jaćimović, Y.-H. Yim, Application of k_0 -INAA method in preliminary characterization of KRISS urban airborne particulate matter certified reference material, Appl. Sci. 10 (19) (2020) 6649.
- [23] K.B. Dasari, H. Cho, R. Jaćimović, G.-M. Sun, Y.-H. Yim, Chemical composition of Asian dust in Daejeon, Korea, during the spring season, ACS Earth Space Chem. 4 (8) (2020) 1227–1236.
- [24] R. Jaćimović, A. Trkov, P. Stegnar, Error in k_0 -NAA measurement due to temporal variation in the neutron flux in TRIGA Mark II reactor, J. Radioanal. Nucl. Chem. 294 (1) (2012) 155–161.